SPIE Int. Symposium on Law Enforcement Technologies, Boston, Massachusetts, USA, 5–8 November 2000, Proc. SPIE 4232

# Model-based analysis of striation patterns in forensic science

M. Heizmann and F. Puente León

Institut für Meß- und Regelungstechnik, Universität Karlsruhe (TH),
Postfach 6980, D-76128 Karlsruhe, Germany

### ABSTRACT

We present a new image processing strategy that enables an automated extraction of signatures from striation patterns. To this end, a signal model is proposed that allows a suitable description of the interesting features of forensically relevant striation marks. To provide for a high image quality, several images of the same surface area are recorded under systematically varying conditions. The images obtained are then combined to an improved result by means of appropriate sensor fusion techniques. Based upon the signal model, the signal of interest is concentrated, and a compact representation of the grooves is obtained. To enable an efficient description of the relevant features even in the cases of deformed surfaces or curved striation marks, a straightening of the grooves is performed before. In the following, a meaningful signature describing the information of interest is extracted using the whole length of the grooves. This signature can be used for an objective evaluation of similarity of striation patterns.

**Keywords:** automated visual inspection, image processing, sensor fusion, striation patterns, toolmarks, firearm bullets, image models, groove straightening, forensic science

## 1. INTRODUCTION

The analysis of marks that have been found at crime plays an essential role within forensic science. For a long time, the groove structures on the circumferential surface of bullets have been used to identify several bullets fired from the same gun or to recognize the appropriate gun for a given bullet. In case of toolmarks, which are often found in case of burglaries and thefts, groove-like textures also arise due to the motion of the tool relative to the touched object.

Archiving such marks for subsequent comparisons results in enormous databases, which can contain some 1,000 marks of the same kind. To perform a reliable analysis, an exhibit showing the mark has to be compared with the entire database. Up to now, this comparison is mainly done by experts visually by means of a comparison macroscope. Because of the large amounts of visual comparisons which are necessary to search the database, the current matching methods for striation patterns are often unable to provide the turnaround times and success rates that law enforcement demands.

Due to these problems, it is desirable to automate the comparison of the marks by means of digital image processing. Here, the computer should not primarily serve to visualize the recorded images, but rather to perform a first comparison in order to assist the expert. The automatic inspection comprises the following steps:

- a digital recording of each mark with adequate conditions during the image acquisition,
- a preprocessing in order to simplify further steps,
- the extraction of suitable features,
- and finally, a comparison with the entire database.

Considering the nature of the marks in the present case, every step has to be adapted to the specific properties of groove-like textures. Stepping up to this challenge, we present in this paper a new image processing strategy that enables an automated extraction of a meaningful signature from the texture. Based on the signatures obtained, an objective and quantitative comparison of striation patterns can be achieved.[14,15]

The basis of this strategy is a novel signal model which is presented in Sect. 2. Considering the signal properties, powerful strategies for the image acquisition and preprocessing can be applied to obtain images of high quality; see Sects. 3 and 4. After that, the proposed signal model is used to robustly extract the signature of the toolmark, as shown in Sect. 5.

Further author information:
Email: {heizmann, puente}@mrt.mach.uni-karlsruhe.de; WWW: http://www-mrt.mach.uni-karlsruhe.de;
Telephone: +49-721-608-{2338, 3604}; Fax: +49-721-661874

## 2. SIGNAL MODEL

Neither bullets nor toolmarks show random collocations of groove-shaped marks. In fact, such textures comply with definite rules which are implicitly met at the time of the generation of the grooves. Individual features of the tool edge or the gun barrel generate the groove-like structures by their relative motion to the surface which bears the toolmark. Therefore, all fluctuations of the gray levels along the grooves are bound to represent disturbances that can efficiently be suppressed by means of a projection in the direction of the grooves. At the same time, the achieved concentration of the information of interest leads to a considerable data reduction, which contributes to an efficient implementation of the later comparison algorithms. Regarding the kinematics of the groove generation, one has to distinguish between marks on pristine bullets on the one hand, and marks on deformed bullets and toolmarks on the other hand.

### 2.1. Pristine Bullets

At the time of firing, the kinematics provides for the generation of straight grooves on the circumferential surface of the bullet. All individual characteristics of the barrel are represented by strictly parallel grooves. Due to the twist of the bullet compared to the direction of flight $\mathbf{e}_y$, the direction $\mathbf{e}_\xi$ of the grooves is inclined with the pitch angle $\psi$; see Fig. 1. Moreover, the direction of a "virtual" edge $\mathbf{e}_\mathrm{e}$ caused by the projection of the characteristics of the barrel is identical to the global direction $\mathbf{e}_x$.

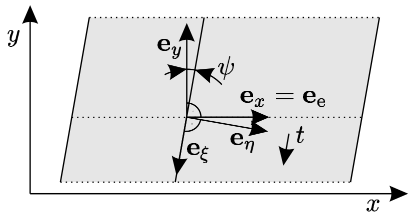


**Figure 1.** Signal model for bullet grooves.

However, curved grooves may also occur on firearm bullets. The described assumption of straight grooves may not always be reasonable, especially with bullets that were heavily deformed at the impact. In that case, one is concerned with signal models which are much more difficult to handle, and which are of importance particularly for toolmarks.

### 2.2. Deformed Bullets and Toolmarks

In case of toolmarks and deformed bullets, the matters are more difficult than with pristine bullets. In general, groove structures occur that cannot be designated as rectilinear. Here, one has to go more closely into the creation of the grooves.

The creation process of groove-like toolmarks reveals that the two-dimensional surface structure emerges from the combined translation and/or rotation of a one-dimensional structure $g(s)$. With respect to toolmarks, this one-dimensional structure corresponds with the tool edge. In reality, the edge may have a spatial character, but due to the small extent of the tool perpendicular to the edge direction, it is usually possible to assume a one-dimensional edge.

In case of deformed bullets, the motion inside the gun barrel causes a projection of the individual features on a "virtual" edge that leaves strictly straight grooves on the bullet. Here, the curvature of the grooves stems rather from the later deformation of the entire bullet than from the groove generation process.

Therefore, the application of a signal model based on a unidimensional, locally constant generation profile requires some assumptions:

- First of all, regarding the acquisition of images $d(\mathbf{x})$, where $\mathbf{x} = (x, y)^\mathrm{T}$ denotes the spatial coordinates, the illumination and the direction of observation have to be kept constant in relation to the groove direction. Consequently, to record images of different marks, all the illumination and positioning parameters should be adjusted exactly and reproducibly.[14]

- Secondly, the marks should be available over a long distance and with their full width in order to robustly estimate the parameters of the signal model. Thereby the application of the signal model can efficiently show its advantages for the suppression of disturbances.

- It has to be made sure that no overlaps of the grooves occur. This means that the tool edge should touch only once a particular location on the surface. With respect to the shape of the grooves, this condition requires continuous paths of all grooves.

- The path of the tool should possess a continuous first derivation. Although this condition seems to be too restrictive, the mass of the tool will in most cases cause differentiable grooves.

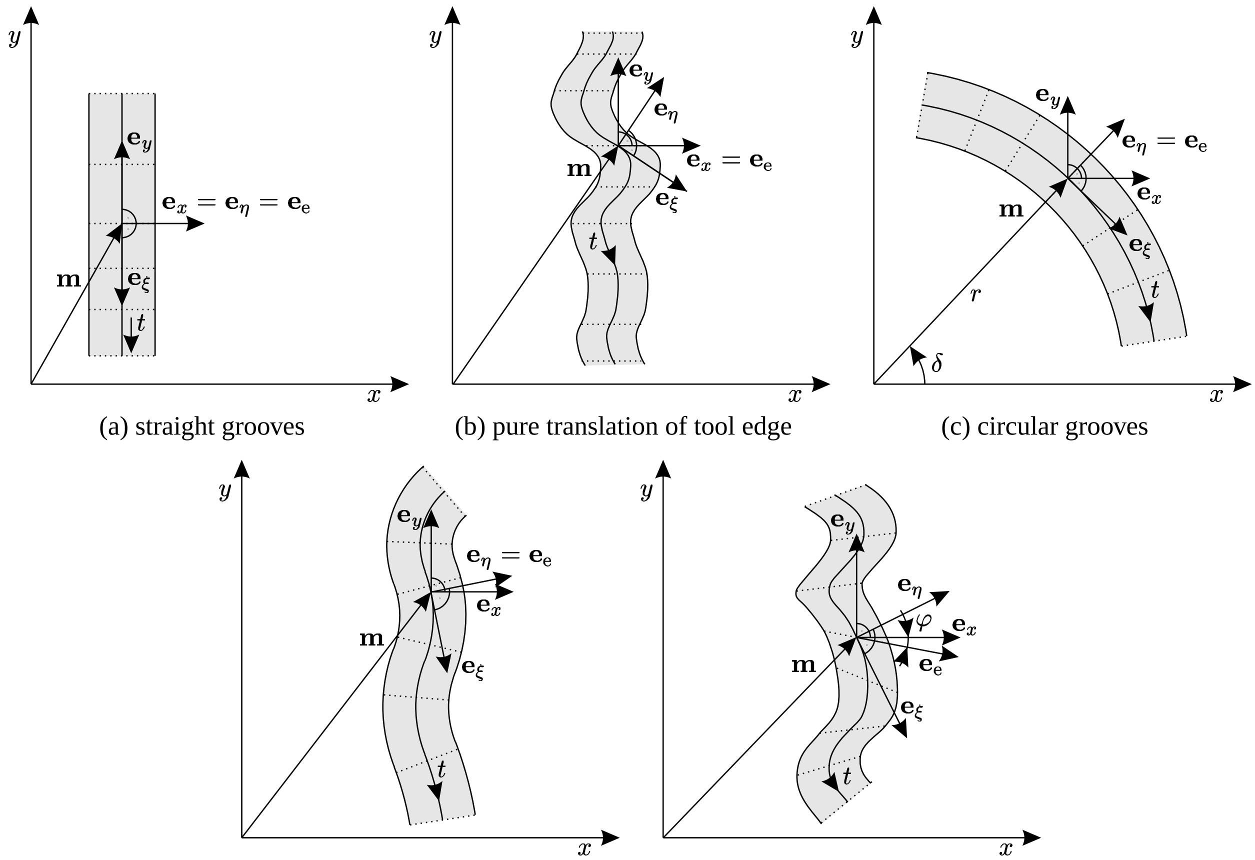


(a) straight grooves (b) pure translation of tool edge (c) circular grooves

(d) piecewise circular grooves (e) arbitrary translation and rotation of tool edge

**Figure 2.** Model mechanisms for generation of grooves.

- Finally, the groove profile has to comply with the requirement of local stationarity. The edge profile is only allowed to alter slowly along the grooves. Such an alteration of the edge profile occurs, for example, when the clearance angle of the tool is changed during the generation of a groove. A reasonable procedure for groove structures showing profile changes would be to split up the entire structure into several sectional structures and to assume a constant groove profile separately for each section.

Various signal models that lead to such groove structures are conceivable. Some examples are depicted in Fig. 2. Each signal model uses as model parameters the curve $\mathbf{m}(t)$ with the curve parameter* $t$ of an arbitrary position on the edge as well as the width of the edge $w$. Besides, specific model parameters are necessary in each case, e.g. in the case of circular grooves (Fig. 2(c)), the center position and the radius of curvature $r$ are needed. Depending on the signal model, correspondences of the local coordinate system $(\mathbf{e}_\xi, \mathbf{e}_\eta)$ in groove direction with the local edge direction $\mathbf{e}_\mathrm{e}$ or the global coordinate system $(\mathbf{e}_x, \mathbf{e}_y)$ are obtained.

With the above mentioned conditions, the gray level function $g^{\mathrm{II}}(\mathbf{x})$ of the groove structure within the image $d(\mathbf{x})$ is obtained from the relation

$$g^{\mathrm{II}}(\mathbf{x}) = g\Big[\big(\mathbf{x} - \mathbf{m}(t(\mathbf{x}))\big)^{\mathrm{T}} \cdot \mathbf{e}_\mathrm{e}\Big] \cdot \mathrm{rect}\left[\frac{\big(\mathbf{x} - \mathbf{m}(t(\mathbf{x}))\big)^{\mathrm{T}} \cdot \mathbf{e}_\mathrm{e}}{w}\right], \tag{1}$$

where $g(s)$ denotes the groove profile in the direction $\mathbf{e}_\mathrm{e}$ of the edge, and

$$\mathrm{rect}(x) = \begin{cases} 1 & \text{for} \quad x \in \left[-\frac{1}{2}, \frac{1}{2}\right] \\ 0 & \text{otherwise} \end{cases} . \tag{2}$$

*The curve parameter $t$ may be, but needs not be identical to the running length.

In some cases, the general relation of Eq. (1) may be simplified. In the case of circular grooves, the simplification $\mathbf{e}_\eta = \mathbf{e}_\mathrm{e}$ with the origin laid in the center of the circle, see Fig. 2(c), yields

$$\mathbf{m}(\mathbf{x}) = r \cdot \mathbf{e}_\eta(\mathbf{x})\,, \tag{3}$$

and with the Euclidean norm $\|\ldots\|$, the following expression is obtained:

$$g^{\mathrm{II}}(\mathbf{x}) = g\left(\mathbf{x}^\mathrm{T} \cdot \mathbf{e}_\eta - r\right) \cdot \mathrm{rect}\frac{\|\mathbf{x}\| - r}{w}\,. \tag{4}$$

Such simplifications can be stated for the first four signal models of Fig. 2. However, the resulting equations cannot be transferred to another signal model. Therefore, an individual method for the recognition of the course of the grooves has to be developed explicitly for each signal model.

The most general signal model is the one in which an arbitrary translation and rotation of the tool edge is permitted; see Fig. 2(e). The only feature that is used in this signal model is that the grooves are generated by a unidimensional, solid edge. If one was able to reconstruct from the recorded image the path $\mathbf{m}(t)$ of a particular point on the edge, and a corresponding edge angle, e.g. $\measuredangle\,(\mathbf{e}_x, \mathbf{e}_\mathrm{e})$, then every image point within the groove structure could be assigned to a particular point on the edge. To some extent, this method would constitute the inversion of Eq. (1).

## 3. IMAGING

In forensic science, the requirements concerning the quality of the images to be evaluated are especially high. To provide for a reliable comparison of forensic marks, a reproducible imaging even of the finest individual marks is necessary. Therefore, great strides must be made in the area of image capture. Ideally, the requirements to be fulfilled by the image acquisition system comprise

- a high-quality image acquisition providing for high contrast, high resolution, high image sharpness, and high signal to noise ratio (SNR) in the whole image,
- a thorough coverage of the surface containing the marks of interest,
- an easily reproducible recording situation,
- and finally, a mostly automated image acquisition.

Due to the limitations of optical systems, illumination problems as well as difficulties in imaging all interesting areas simultaneously and with the required resolution, it is often not possible to meet all these requirements with only one image $d(\mathbf{x})$ of the object; see Figs. 3(a) and (b). Instead, these requirements can be fulfilled by acquiring several images under different recording conditions. If attention is paid to a proper choice of the degrees of freedom of the image acquisition system, and its parameters are varied systematically, the images obtained can then be combined to an enhanced result $r(\mathbf{x})$ matching all requirements, upon which the further processing can be based.[†] An example of such an image is shown in Fig. 3(c).

A strategy to generate suitable images $r(\mathbf{x})$ consists in recording a series of images

$$\mathcal{D} = \{d(\mathbf{x}, \boldsymbol{\omega}_i),\ i = 0, \ldots, B-1\} \tag{5}$$

in which the object distance, the illumination direction, and the object pose are all varied, and a subsequent multidimensional image fusion is performed.[3,6] The image series $\mathcal{D}$ is characterized by a parameter vector

$$\boldsymbol{\omega} = (\phi, \theta, \zeta, \boldsymbol{\alpha}^\mathrm{T}, \ldots) \tag{6}$$

describing the acquisition situation, where $\phi$ and $\theta$ represent the azimuth and the elevation angle of the illumination direction, respectively, $\zeta$ denotes the object distance, and $\boldsymbol{\alpha}^\mathrm{T}$ the object pose with respect to the imaging system. Of course, additional parameters—such as the integration time of the camera or the wavelength of the illumination source used—could be varied too, if necessary. However, in this paper we will focus on illumination problems, because they play a crucial role in imaging of groove structures.[12] For more information on the impact of other image acquisition problems as well as on strategies to compensate them, see Refs. 13, 14, and 16.

[†]In some particular cases, more than a single resulting image will be necessary to describe the marks of interest in their entirety. However, such cases concern constellations of marks showing a complex geometry, and they will not be considered in this paper.

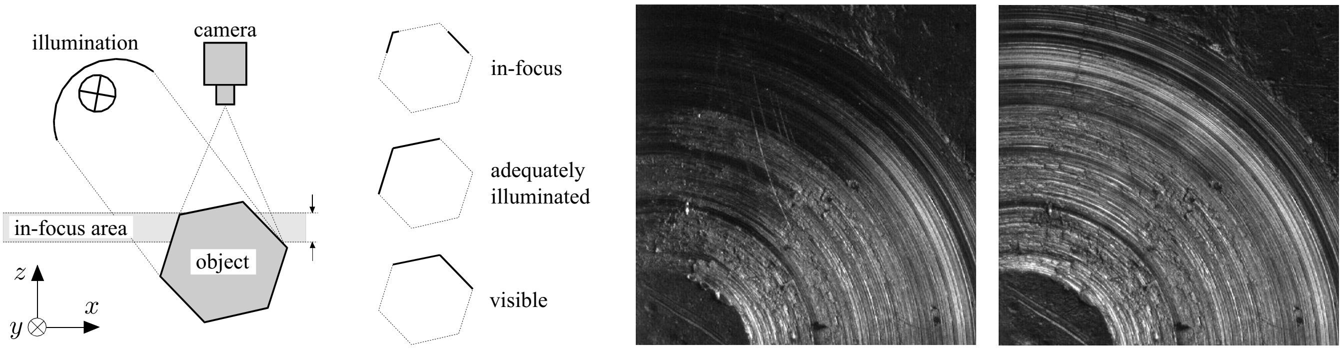


(a) (b) (c)

**Figure 3.** Image acquisition problems: (a) general scheme; (b) example of an inhomogeneous image of a toolmark according to model Fig. 2(c) obtained with directional lighting; (c) enhanced image obtained by fusion methods.

### 3.1. Image capture

To image surface textures showing marks with high contrast, a suitable illumination has to be chosen. It can be shown that the image intensities obtained from such surfaces highly depend on the direction of the light source, if directional lighting is used; see Fig. 3(b).[12] Since a diffuse illumination pattern can be thought of as a superposition of many single directional light sources from different directions, diffuse lighting will generally lead to a contrast attenuation, and thus to suboptimal results. However, although directional lighting is preferable to illuminate subtle surface structures, the position of the light source will have to be adjusted for each location $\mathbf{x}$ of the surface, if an optimal local contrast is wanted.

An important question when recording an image series deals with the strategy for sampling the parameter space $\boldsymbol{\omega}$ with as few images as possible such that (1) every surface location $\mathbf{x}$ is imaged with high quality in at least one image of the series, and (2) fusion to an improved result $r(\mathbf{x})$—like e.g. the one shown in Fig. 3(c)—is possible. This problem highly depends on the object geometry as well as on the surface texture and cannot be dealt with in detail here. However, the following some cases relevant to forensic applications will be treated in more detail:

- **Circumferential surface, straight grooves:** To record image series of circumferential surfaces showing a single band of straight, parallel grooves, like e.g. pristine bullets, it is not necessary to vary the illumination space two-dimensionally, because such surfaces only show a high contrast if illumination is perpendicular to the grooves.[12] Thus, only the elevation angle $\theta$ has to be varied. If the interesting surface areas are not all in-focus simultaneously, the object distance $\zeta$ should be varied, too.
- **Plane surface, curved grooves:** In case of plane surfaces consisting of curved grooves, it is usually sufficient to record an image series in which the azimuth $\phi$ is varied. This case is typical for a wide range of forensically relevant marks generated by screwdrivers and other tools.
- **Curved surface, curved grooves:** In the most complicated case of curved surfaces containing curved grooves, such as deformed bullets, the elevation angle $\theta$ as well as the azimuth $\phi$ of the light source have to be varied to assure a high quality in at least one image of the series. Additionally, also the object distance $\zeta$ and the object pose $\boldsymbol{\alpha}^{\mathrm{T}}$ may have to be varied as well to provide for a proper focusing and low distortions.

### 3.2. Fusion strategy

After an image series $\mathcal{D}$ has been acquired, a suitable strategy has to be applied to combine the information of interest distributed over the series to an enhanced result $r(\mathbf{x})$ showing overall a high quality. Such a result is not only advantageous to enable a computerized comparison, but it can also be used to support forensic examiners in matching of striae, because a larger area of the surface can be visualized with high contrast simultaneously than when using conventional tools like comparison macroscopes.

In this paper, only one-dimensional illumination series—i.e. series in which only one illumination parameter is varied—will be discussed. However, by applying this method in several stages, multidimensional series of images can also be fused.[12] Fig. 4 shows the structure of the fusion algorithm for the case of a varying azimuth $\phi$.

The fusion algorithm is based on the selection of the best illuminated image segments of the series for each location $\mathbf{x}$ based on a the maximization of a local criterion $C$. Since in our case a high contrast is desired, the local gray level variance and the

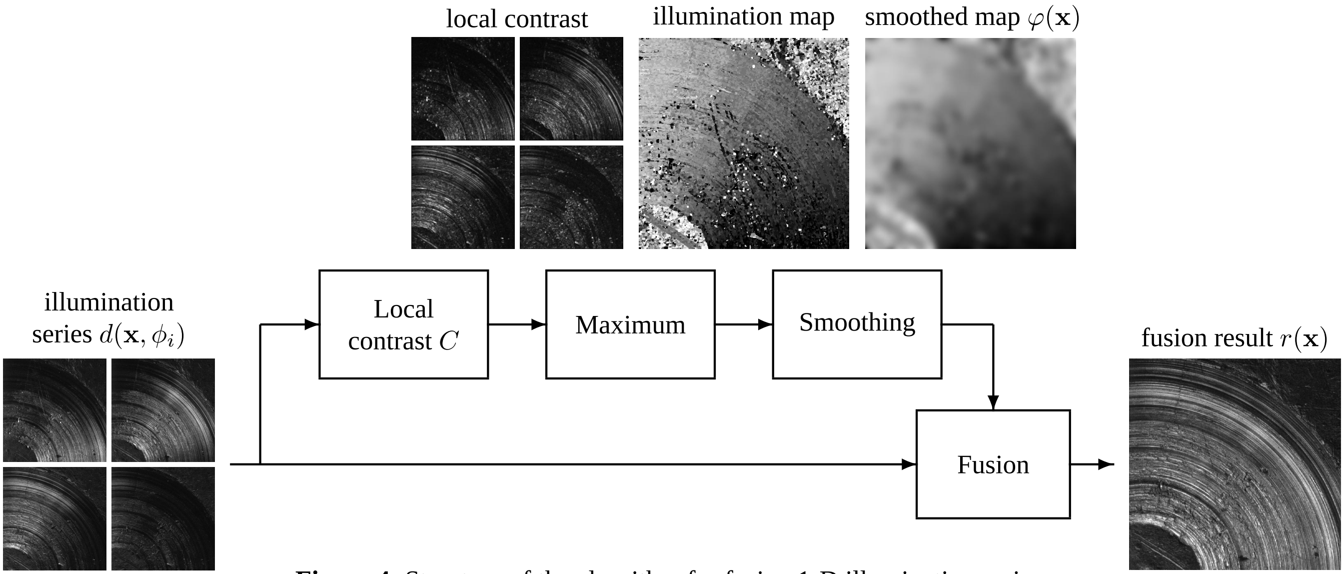


**Figure 4.** Structure of the algorithm for fusing 1-D illumination series.

local entropy are suitable options to compute the local criterion $C$. The selected illumination direction maximizing the contrast, which is stored for each location $\mathbf{x}$ in the so-called *illumination map*

$$\tilde{\phi}(\mathbf{x}) = \arg\max_{\phi_i} C\{d(\mathbf{x}, \phi_i)\}\,, \tag{7}$$

has to be a spatial function varying slowly compared with the signal of interest, i.e. the width of the grooves. This is necessary to avoid artifacts in the fusion result. To assure that this condition is satisfied, a smoothing of the illumination map with a binomial low-pass filter is performed:[7]

$$\varphi(\mathbf{x}) = \angle \mathrm{LP}\{\exp(\mathrm{j}\tilde{\phi}(\mathbf{x}))\}\,. \tag{8}$$

In this step, the cyclicity of $\phi$ has to be taken into account, because the equation $\phi = \phi + 2\pi k$, $k \in \mathbb{Z}$, holds. Thus, not $\tilde{\phi}(\mathbf{x})$ itself, but the complex pointer $\exp(\mathrm{j}\tilde{\phi}(\mathbf{x}))$ has to be smoothed. The resulting function $\varphi(\mathbf{x})$, which denotes the best-suited local illumination direction, is the angle of the complex result.[11]

The actual fusion is performed by a weighted superposition of two adjacent images $d(\mathbf{x}, \phi_i)$ by means of a linear interpolator $\gamma$ taking the best local illumination direction $\varphi(\mathbf{x})$ into account:

$$r(\boldsymbol{x}) = \frac{(\varphi(\boldsymbol{x}) - \phi_k) \bmod 2\pi}{(\phi_l - \phi_k) \bmod 2\pi}\, d(\boldsymbol{x}, \phi_k) + \frac{(\phi_l - \varphi(\boldsymbol{x})) \bmod 2\pi}{(\phi_l - \phi_k) \bmod 2\pi}\, d(\boldsymbol{x}, \phi_l) \tag{9}$$

with

$$l := (k+1) \bmod B\,, \qquad (\phi_l - \phi_k) \bmod 2\pi \leq (\varphi(\boldsymbol{x}) - \phi_k) \bmod 2\pi\,.$$

The interpolation takes care of a smooth transition between $\phi$-neighboring images. The narrow extent of $\gamma$ provides for an averaging of only similarly illuminated images. Thus, an undesirable contrast loss due to destructive interferences of light and shadow in different images of the series is avoided.

Three properties of the proposed fusion method are responsible of its good performance:

1. the fusion result $r(\mathbf{x})$ resembles locally the best illuminated image $d(\mathbf{x}, \phi_i)$ of the series;

2. the smoothness of the selected illumination direction $\varphi(\mathbf{x})$ guarantees that no artifacts are contained in the resulting image $r(\mathbf{x})$;

3. the resulting image achieves globally good results in the sense of maximizing the local contrast $C$.

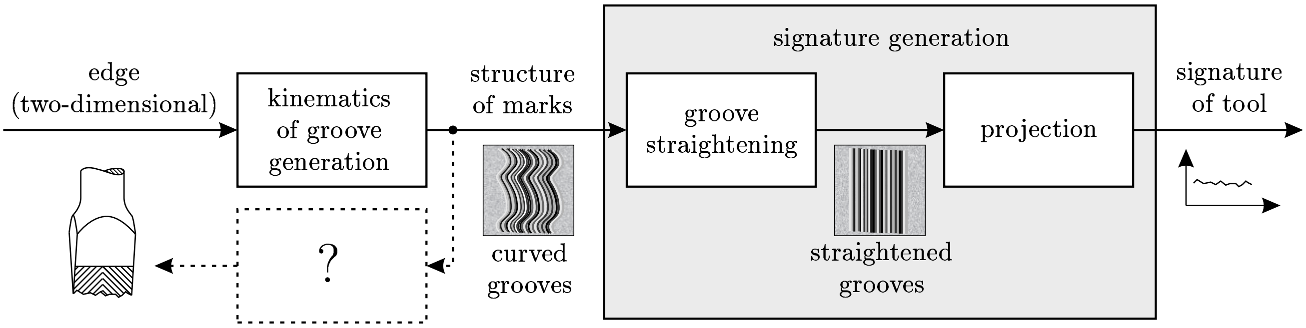


**Figure 5.** Groove straightening and generation of a signature.

A fusion of an image series in which the elevation angle $\theta$ of the illumination direction is varied can be performed in an analog manner. However, since the elevation angle $\theta$ is not cyclic, instead of Eq. (9) the following simplified expression is obtained:

$$r(\mathbf{x}) = \sum_i d(\mathbf{x}, \theta_i)\gamma(\vartheta(\mathbf{x}) - \theta_i) = \frac{\vartheta(\mathbf{x}) - \theta_l}{\theta_{l+1} - \theta_l} d(\mathbf{x}, \theta_l) + \frac{\theta_{l+1} - \vartheta(\mathbf{x})}{\theta_{l+1} - \theta_l} d(\mathbf{x}, \theta_{l+1}) \qquad (10)$$

with

$$\vartheta(\mathbf{x}) = \mathrm{LP}\{\tilde{\theta}(\mathbf{x})\}\,, \qquad \tilde{\theta}(\mathbf{x}) = \arg\max_{\theta_i} C\{d(\mathbf{x}, \theta_i)\}\,.$$

## 4. PREPROCESSING

After having generated a high-quality image showing the marks of interest by means of the fusion approach presented in Subsect. 3.2, a preprocessing of this image is performed to suppress texture inhomogeneities that arise from the illumination process and from the object shape. At the same time, the further signal processing steps will be simplified. For this purpose, a directional Gaussian high-pass filter is used which eliminates slowly varying gray level fluctuations perpendicular to the grooves and provides for a homogenization of first degree[‡]—i.e. of the local average gray level—without generating undesirable artifacts.[1,10]

Alternatively, a homogenization of second degree, in which the local contrast is equalized as well,[1] was also tested. However, since this powerful homogenization method leads to a significant alteration of the signal of interest, it appeared to be a less indicated preprocessing tool for quantitative image comparison.[14]

## 5. GENERATION OF A SIGNATURE

To provide for an efficient computerized comparison of marks, it is desirable not to use the preprocessed two-dimensional images for this task. Instead, a data reduction should be performed first that gains from the image a *signature*, that means a unidimensional "fingerprint" of the groove structure on the toolmark. The resulting signature can then be considered characteristic for a certain specimen of a tool.

The proposed signal model of Sect. 2 bases on the kinematic relations that are imposed during the generation of grooves. In so far, it would be ideal, if one was able, by means of the kinematics, to conclude the unidimensional edge directly from the recorded image of the marks. This would represent the inversion of the kinematics during the groove generation; see Fig. 5. However, such an immediate strategy seems not to be feasible, as usually—except while preparing sample toolmarks for comparison reasons—the kinematics of the groove generation is not known. Therefore, it is necessary to extract the signature without prior knowledge of parameters concerning the kinematics.

Many of the strategies applied up to now to obtain such signatures use a single profile of the groove structure which is placed perpendicular to the groove direction.[4,5,9] Sometimes, a small quantity of interactively specified profiles is averaged. In general, a computerized and automated optimization of the parameters determined thereby (e.g. the angle to the local direction of the grooves) is not performed.

[‡]In image processing literature, this step is often referred to as a shading correction.

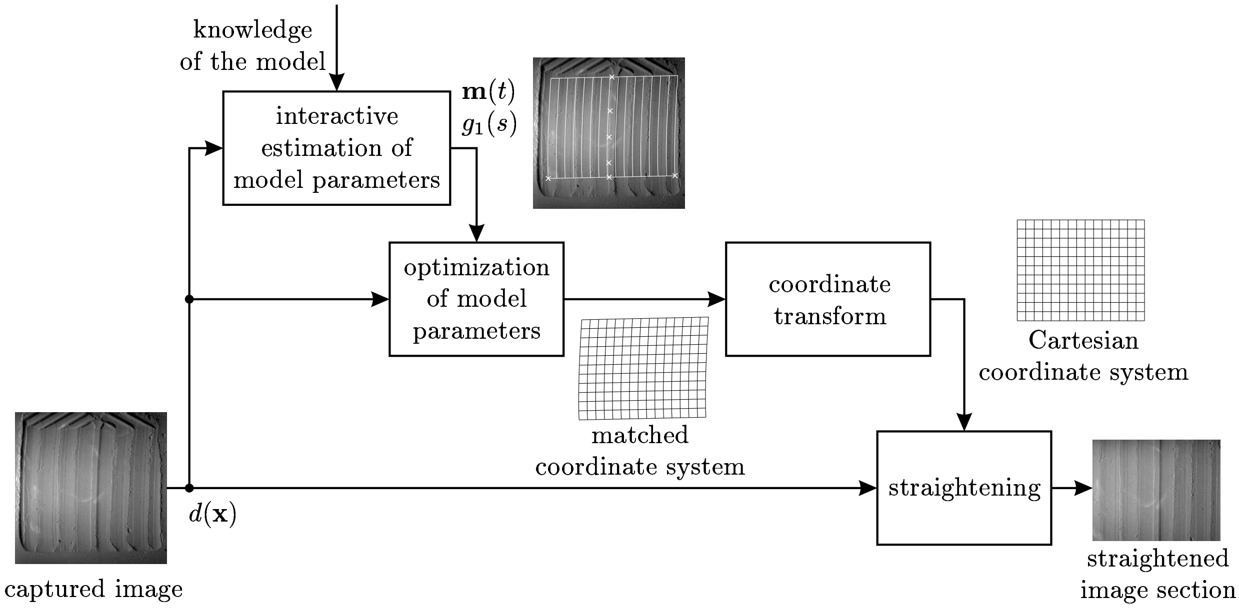


**Figure 6.** Model-based groove straightening algorithm.

The important drawback of these strategies concerns their high susceptibility to all kinds of disturbances. The groove texture of a mark may be disturbed by various factors, e.g. by subsequently introduced scratches, by soiling, but also by cavities and inclusions when castings are used. Therefore, a robust strategy to trace and straighten grooves is proposed below.

The underlying idea is that considering the whole length of the groove offers a substantial possibility to suppress the influence of local disturbances on the resulting signature. Since local disturbances affect only minor regions of the marks, a suitable filtering along the grooves can reduce their influence. Filtering the gray values along a groove yields one point of the signature. Repeating the groove tracing for all grooves of the texture, the desired signature is obtained.

### 5.1. Pristine Bullets

Considering strictly straight grooves, which occur on pristine bullets or—in rare cases—on toolmarks, the proposed strategy can easily be illustrated. Taking the applicable signal model into account (Figs. 1, 2(a)), the global pitch angle $\psi$ determines the global direction of the grooves. Therefore, this angle has to be estimated in order to perform the projection along the direction of the grooves. To estimate this global parameter, suitable algorithms are available, e.g. those based on the evaluation of the periodogram of the recorded groove patterns.[14]

### 5.2. Deformed Bullets and Toolmarks

If the local orientation of the grooves changes within the interesting area, the consideration of the whole length of the grooves turns out more complicated. Here, every image point has to be assigned individually to a particular position on the unidimensional edge. The grooves have to be traced along the whole area of the mark. In this case, suitable strategies comprise a local orientation analysis and model-based methods.

**Local orientation analysis:** Independently of the origin of a groove texture, the local direction of a groove can be determined by means of local features. Thereby, the methods base e.g. on the directional dependence of the variance or gradients of gray values as well as on directionally dependent Fourier analysis. Such methods have been developed and tested at the Institut für Meß- und Regelungstechnik.[14] In many cases of technically relevant textures like e.g. end-milling textures, a local orientation analysis of sufficient quality can be performed and applied for purposes of quality assurance. The methods have also been successfully analysed and applied to the processing of traces on deformed bullets.

However, a reliable identification of the local groove direction demands that the texture of the considered surface shows a sufficiently pronounced preferential direction in local regions. Concerning the processing of toolmarks, a segmentation of the texture into regions containing grooves and background regions has to be performed first. Moreover, strong effects come from

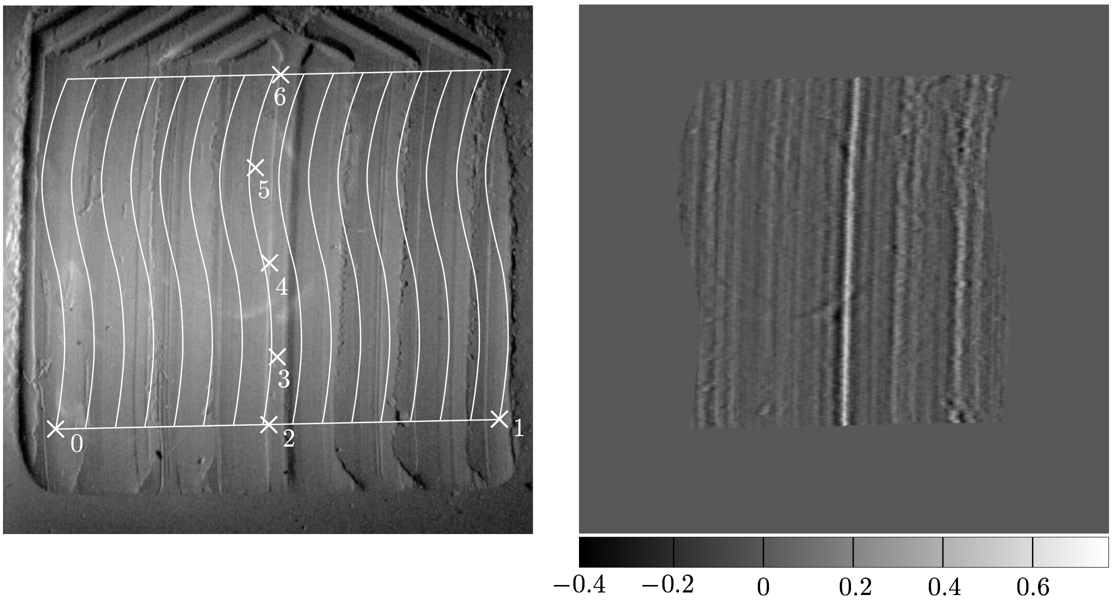


(a) (b)

**Figure 7.** Groove straightening: (a) interactive estimation of the guiding groove; (b) respective correlation image.

the property of toolmarks that they often do not show sufficiently pronounced grooves over the whole width of the marks. This leads to local defects of the orientation analysis, which considerably reduces the usability of this method.

**Model-based groove tracing:** With model-based strategies for groove straightening, a suitable signal model of Sect. 2 allows to conclude the path of the edge from the arrangement of the grooves in the image. The algorithm for a model-based approach is depicted in Fig. 6, with marks generated by a pure translation of the tool edge. Marks described by other suitable signal models—and appropriately adapted model parameters—can be treated analogously.

Starting from the preprocessed image $d(\mathbf{x})$, an adequate signal model has to be chosen. The knowledge of the underlying signal model determines the definition of the model parameters. Concerning the example of Fig. 6, the assumption of a pure translation of the tool edge (Fig. 2(b)) seems to be suitable. For this signal model, an *edge line* ($g_1(s)$), which describes the direction and the width of the edge, and a *guiding groove* ($\mathbf{m}(t)$) are required as model parameters. Thereby, the arguments $s$ and $t$ describe the position in the direction of the edge and the curve parameter, respectively.

Firstly, the two model parameters—edge line and guiding groove—are estimated interactively by the forensic examiner; see Fig. 7(a). Here, the edge line is defined as the width of the interesting region of the mark in the assumed edge direction (points 0, 1). Furthermore, the guiding groove is estimated manually. For that purpose, several points on a particularly pronounced groove are marked. To achieve a smooth path describing the marked groove, the points are interpolated by means of *splines* (points 2–6). However, it does not seem to be adequate to estimate the path of the grooves exclusively in an interactive manner for some reasons:

- A sufficiently precise groove tracing often suffers from the interactive localization.
- For reasons of reliability and reproducibility, any unsupervised adoption of interactively determined data should be avoided.

To solve these difficulties, a computer-aided optimization of the guiding groove based on the interactive estimation is performed. Several approaches are available for this task. In the following, an algorithm is presented that performs an optimization of the position of all points on the discrete guiding groove by means of a direct maximization of the local correlation coefficient.

Alternatively, the guiding groove can be regarded as an active contour (*snake*).[8] With some slight adaption concerning the definition of the internal energy, such a snake can be fitted to the optimal groove path by using known methods. Furthermore, the application of snake algorithms to the control points of a spline describing the guiding groove constitutes another possibility.[2]

The advantage of approaches based on snakes consists in the implicit consideration of continuity conditions. On the other hand, they entail a significantly increased computational expense.

The cross-correlation function (CCF) is a well-known tool to detect linear correspondences. In forensic science, its application to matching patterns of striae also provides successful and robust results.[14] The CCF is defined as

$$k_{12}(\tau) := \tilde{g}_1(s) \circledast \tilde{g}_2(s) = \int_{-\infty}^{\infty} \tilde{g}_1(s) \cdot \tilde{g}_2(s+\tau)\, \mathrm{d}s\ , \tag{11}$$

where the signals $g_1(s)$ and $g_2(s)$ are standardized by centering them around their mean values $m_{g1}$, $m_{g2}$ and dividing them by their standard deviations $s_{g1} = \sqrt{\mathrm{var}\{g_1\}}$, $s_{g2} = \sqrt{\mathrm{var}\{g_2\}}$, respectively:

$$\tilde{g}_1(s) = \frac{g_1(s) - m_{g1}}{s_{g1}}\ , \qquad \tilde{g}_2(s) = \frac{g_2(s) - m_{g2}}{s_{g2}}\ . \tag{12}$$

Then, the value of the maximum $\rho_{12} := \max\{k_{12}(\tau)\}$ stands for the degree of similarity between both signals. The nearer $\rho_{12}$ lies to the maximal value 1, the stronger the resemblance is. The maximum position of the CCF

$$\tau_0 := \arg\max_{\tau} \{k_{12}(\tau)\} \tag{13}$$

supplies the information, how far the signals have to be shifted against each other in order to achieve a matching of both signals.

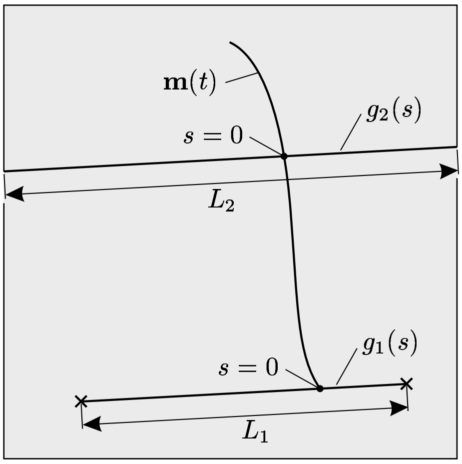


**Figure 8.** Signals $g_1(s)$ and $g_2(s)$.

To obtain the signal $g_1(s)$, the gray values on the chosen edge line are taken; see Fig. 8. This signal serves as a reference pattern for the following correlation. According to its interactive definition, it is spatially limited and has the length $L_1$. It might be reasonable to limit the region around the marked groove, e.g. by means of a Gaussian function $G(s, \sigma)$. Thus, a higher weight of the center region is obtained in comparison to more distant parts. Since defects of the groove pattern are more likely to appear at the border of the mark, their influence on the CCF is thus reduced. The advantage of neglecting remote parts of the groove is easy to understand, as the guiding groove is chosen as a groove which can be easily traced. The origin of $g_1(s)$ is positioned on the guiding groove. For every image point on the interactively defined guiding groove $\mathbf{m}(t)$, the corresponding signal $g_2(s)$ is determined as the gray levels along the straight line parallel to the edge line through $\mathbf{m}(t)$. The origin $g_2(s = 0)$ is also set on the guiding groove. In contrast to $g_1(s)$, the length $L_2$ of the signal $g_2(s)$ is not limited to a defined value. $L_2$ only depends on the image boundaries.

Now the maximum position of the CCF is located at the optimal shifting value, where the groove profile $g_2(s)$ shows the highest similarity to the reference profile $g_1(s)$. If the maximum position deviates from $\tau_0 = 0$ for a certain point $\mathbf{m}(t)$, the guiding groove has to be shifted at that very point by the amount $\tau_0$ in the direction of the edge line to correct the error caused by its interactive estimation.

To give an example, Fig. 9 depicts two signals extracted from a toolmark and their cross-correlation function $k_{12}(\tau)$. First of all, the recorded image has been locally normalized by means of an operator $\mathcal{H}_1\{.\}$ performing a homogenization of first degree.[1,14] After that, a Gaussian function has been used to limit the signal $g_1(s)$ spatially. The CCF shows a strongly pronounced maximum with $\rho_{12} = 0.43$. Although this value would seem to be quite low for other applications based on the CCF, the only important property in this context is a reliable identification of the global maximum. In this respect, the obtained value is sufficient for a further evaluation.

The CCFs that have been calculated at every position of the guiding groove can be coded as gray values and assembled as a correlation image; see Fig. 7(b). Here, the origin of the CCF is set to the corresponding point on the guiding groove. The shift values $\tau$ are plotted in the direction of the edge line. The maxima $\rho_{12}$ of the CCFs are visible as a light line in the correlation image. Although the guiding groove in the example of Fig. 7 has been described very inaccurately, the CCFs show distinct maxima that faithfully reflect the real path of the guiding groove.

As the result of the optimization, a matched coordinate system is obtained that can be used to perform a straightening of the grooves.

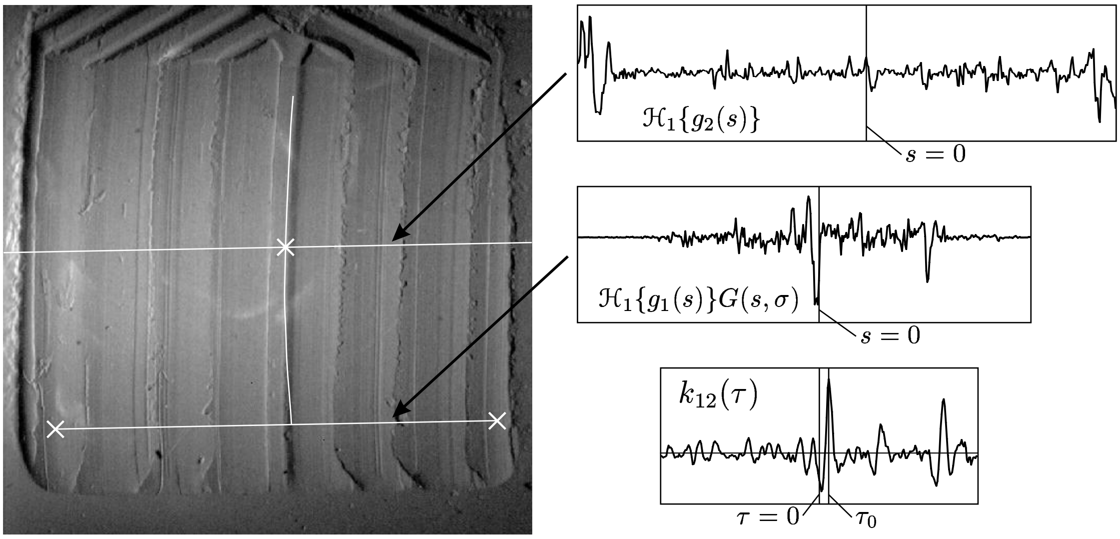


**Figure 9.** Direct correlation.

### 5.3. Groove Straightening

The final step of the model-based strategy is the groove straightening. The optimization of the interactively defined model parameters yields a matched coordinate system, where the groove direction corresponds locally to one of the coordinate directions. The other coordinate direction is not affected by the optimization and represents the edge direction. To perform a conversion of the matched coordinate system into a Cartesian coordinate system, a coordinate transform is defined and applied to the recorded image; see Fig. 6. After that, the resulting image represents the straightened image section. Once the grooves have been straightened, the signature can be computed by performing a projection in the direction of the grooves.

## 6. CONCLUSIONS

In this paper, a model-based description of the structure of a wide range of forensically relevant marks—toolmarks as well as marks on firearm bullets, among others—has been introduced. Aided by this model, a strategy to generate high-quality images of the surfaces containing the marks has been proposed. In order to obtain reliable signatures, a novel methodology to trace and straighten the groove-shaped marks has been discussed. Encouraging results have been presented for the tracing of a toolmark generated by a pure translation of a tool.

Future enhancements of the strategy will focus on grooves showing substantial alterations along their path. Since in such cases—e.g. due to a change of the clearance angle of the tool—the assumption of a unique edge profile is not allowed, multiple signatures have to be extracted. Due to the inertia of the tool, a slow spatial variation of the edge profile can be assumed. Thus, it is straightforward to perform a low-pass filtering along the direction of the grooves, and to obtain several signatures by subsampling the groove texture in that direction. By taking different signatures of a single tool into account, the reliability of the proposed strategy will be significantly increased.

## ACKNOWLEDGEMENTS

The authors would like to thank Dr. Horst Katterwe and Mr. Michael Braune, Bundeskriminalamt, for motivating part of the work presented in this paper, and for providing us with sample toolmarks.

## REFERENCES

1. J. Beyerer and F. Puente León, "Suppression of Inhomogeneities in Images of Textured Surfaces", *Opt. Eng.* **36** (1), 85–93, 1997.
2. R. Cipolla, *Active Visual Inference of Surface Shape*, Springer-Verlag, Berlin, Heidelberg, 1995.
3. J.J. Clark and A.L. Yuille: *Data Fusion for Sensory Information Processing Systems*, Kluwer Academic Publishers, Boston, 1990.

4. W. Deinet, “Studies of Models of Striated Marks Generated by Random Processes,” *Journal of Forensic Sciences* **26** (1), 35–50, 1981.
5. Z. Geradts, J. Keijzer, I. Keereweer, “A New Approach to Automatic Comparison of Striation Marks,” *Journal of Forensic Sciences* **39** (4), 974–980, 1994.
6. X.E. Gros: *NDT Data Fusion*, Arnold, London, 1997.
7. B. Jähne, *Digital Image Processing: concepts, algorithms, and scientific applications*, Springer, Berlin, 1993.
8. M. Kass, A. Witkin, D. Terzopoulos, “Snakes: Active Contour Models,” *International Journal of Computer Vision* **1** (4), 321–331, Kluwer Academic Publishers, 1987.
9. H. Katterwe, K.-D. Grooß, T. Gast, T. Mielke, “Über Gesichtspunkte zur Mustererkennung von Feldereindrücken an Projektilen mit optischen Verfahren,” *Archiv für Kriminologie* **181**, 65–75, 1988.
10. T. Lindeberg, *Scale-Space Theory in Computer Vision*, Kluwer Academic Publishers, Boston, 1994.
11. K.V. Mardia, *Statistics of Directional Data*, Academic Press, London, 1972.
12. F. Puente León: “Enhanced imaging by fusion of illumination series,” In: *Sensors, Sensor Systems, and Sensor Data Processing*, Proceedings of SPIE **3100**, pp. 297–308, 1997.
13. F. Puente León and J. Beyerer: “Datenfusion zur Gewinnung hochwertiger Bilder in der automatischen Sichtprüfung,” *Automatisierungstechnik* **45** (10), 480–489, 1997.
14. F. Puente León: *Automatische Identifikation von Schußwaffen*, VDI Verlag, Düsseldorf, 1999.
15. F. Puente León and J. Beyerer: “Automatic comparison of striation information on firearm bullets,” In: *Intelligent Systems and Advanced Manufacturing*, Proceedings of SPIE **3837**, pp. 266–277, 1999.
16. G.H. Tarbox and S.N. Gottschlich, “Planning for complete sensor coverage in inspection,” *Computer Vision and Image Understanding* **61** (1), 84–111, 1995.